Journal of
Ceramic Science
and Technology

J. Ceram. Sci. Technol., **16** [4] 247-254 (2025)
DOI: 10.4416/JCST2025-00004
available online at: http://www.ceramic-science.com

Effect of Strontium Substitution on the Bioactive Properties and Structure of Borate-Based Bioglass

Chen Yang*, Bo Jia, Fei Wang, Yufei Wang, Wenbo Yang, Li Liang

Xi'an Seal Electronic Material Technology Co., Ltd, Xi'an 710201, China.

received January 22, 2025; received in revised form May 31, 2025; accepted June 3, 2025

Abstract

Borate-based bioglass has attracted keen interest as a bone repair material owing to its good machinability and degradability, but the quick release of boron can lead to cytotoxicity and this is an issue that needs to be taken into consideration. In this paper, borate-based bioglass scaffolds substituted with 0 – 9 mol% strontium with a porous microstructure were prepared by means of a polymer foam replication technique. The effect of the strontium substitute on the bioactive properties and structure of the scaffolds was investigated by means of XRD, SEM, MTT, FTIR and MAS-NMR testing. The results showed that the as-made bioglass was amorphous and had a porous microstructure similar to human trabecular bone. The *in vitro* bioactivity of the glass was observed based on the conversion of the glass surface to a nanostructured hydroxyapatite layer in SBF. The substitution of strontium in borate-based bioglass keeps the concentration of B^{3+} ions in a more acceptable[GS1] range. According to the Fourier transform infrared and MAS-NMR spectra, when the strontium increased, part of the silicate network structure in the glass is destroyed. Meanwhile, the layer structure containing [BO_3] is gradually replaced by the framework structure containing [BO_4], this is the basic reason why the bioactive properties of the borate-based glass changed with the strontium substitution.

Keywords: Borate-based bioglass, strontium, bioactive properties, structure

I. Introduction

The clinical demand for engineered bone tissue has been growing in recent years in direct relation to the increase in the human population [1]. The development of novel bone repair materials to assist patients in recovering from bone defects represents a critical challenge that the field of biomedical materials science is actively addressing. Inspired by the principles of bone tissue engineering, the biomimetic fabrication of bone offers a promising strategy for the regeneration of bone tissue and the restoration of bone defects [2–4]. This approach leverages advanced techniques to replicate the natural microstructure and function of bone, providing a viable pathway for effective tissue repair and regeneration. By integrating innovative materials and methodologies, researchers aim to create solutions that closely mimic the biological properties of natural bone, thereby enhancing the potential for successful clinical outcomes [5]. Bioactive glass as bone repair material has attracted increasing attention on account of its excellent bioactivity, osteoconduction and controllable degradation, and it has been widely used in the biomedical field in certain countries and regions [6].

Bioactive glasses, including the widely studied 45S5 composition and other silicate-based variants, constitute a significant category of inorganic, bioactive biomaterials utilized in the fabrication of scaffolds for bone tissue engineering [7–8]. These materials possess distinctive characteristics that make them particularly suitable for such applications, notably their osteoinductive properties, their capacity to form bonds with both soft and hard tissues, and their ability to generate a carbonated hydroxyapatite (HCA) layer upon contact with biological fluids. The formation of this HCA layer is a critical factor in facilitating robust adhesion between bioactive glasses and human bone tissue, thereby enhancing their integration and functionality within the biological environment [9–10]. Studies have shown that CaO and P_2O_5 in bioglass based on the SiO_2-CaO-P_2O_5 system determine the biological activity of the material, while SiO_2 determines the mechanical strength of the bioglass. However, 45S5 and other silicate-based bioglass are absorbed slowly or undergo incomplete conversion into a bone-like material after *in vivo* implantation, which severely limits the use of bioglass in biomedical applications [11–14].

Borate-based bioglass has demonstrated a higher propensity for degradation comparable to other glass compositions, particularly those based on silicate systems. This characteristic makes borate-based bioglass a more accessible bioactive material for fabricating scaffolds with anatomically relevant geometries [15–16]. Additionally, boron, as an essential trace element, has been identified as a potential stimulant in bone tissue engineering applications [17]. Research indicates that boron plays a role in modulating RNA synthesis within fibroblast cells, further underscoring its biological relevance [18–19].

* Corresponding author: Chen Yang

However, the degradation pathways of borate-based bioglass differ significantly from those of 45S5 bioactive glass, highlighting distinct material behaviors. In a study conducted by Fu *et al.*, it was observed that a boron concentration of 7 ppm in the cell culture medium inhibited cellular growth and proliferation [20]. This finding underscores the importance of considering the relatively low chemical durability of borate-based glasses to mitigate potential toxicity risks associated with excessive boron release. Consequently, careful optimization of the boron content is essential to balance bioactivity and biocompatibility in tissue engineering applications.

Strontium has been suggested as a daily oral supplement for the treatment of osteoporosis and shown beneficial effects on bone cells and bone formation *in vivo* [21]. Based on the structural role of Sr in glass networks, we prepared strontium substitution borate-based bioglass scaffolds with a polymer foam replication method. The borate-based bioglass had a composition designated 13 – 93B2, with a composition identical to silicate 13 – 93 glass but with two-thirds of the molar content of SiO_2 replaced with B_2O_3. In this paper, the effect of SrO as a substitute for CaO on *in vitro* bioactivity, ionic diffusion and the structure of borate-based bioglass was investigated.

II. Experimental

(1) Preparation of borate-based bioglass

The borate-based glass compositions studied in this paper are based on the 13 – 93B2 glass composition ($18SiO_2$, $36B_2O_3$, 22CaO, $6Na_2O$, $8K_2O$, 8MgO, $2P_2O_5$ mol%) with calcium oxide substituted by 0, 3, 6 and 9 mol% strontium oxide and they are named S_0, S_1, S_2 and S_3. A borate-based glass scaffold was prepared with a polymer foam replication method. Appropriate amounts of analytical grade SiO_2, H_3BO_3, $CaCO_3$, Na_2CO_3, K_2CO_3, $MgCO_3$, and $NaH_2PO_4{\cdot}2H_2O$ (Sinopharm Chemical Reagent Co., Ltd. Shanghai, China) were mixed thoroughly and melted in a Pt crucible at 1 300 °C for 2 h, and then immediately quenched in cold deionized water. The particles were further ground for 2 h in an attrition mill using high-purity Y_2O_3-stabilized ZrO_2 milling media and ethanol as the solvent, to produce particles of size 1.0 ± 0.5 μm, as measured by a laser diffraction particle size analyzer. Scaffolds were prepared with a polymer foam replication technique, as described in detail elsewhere [22]. Briefly, polyurethane foam (1 cm × 1 cm × 1 cm) was immersed three times in a slurry obtained by mixing 25 vol% glass powder with PVA binder. The as-coated foam was dried for at least 8 h at room temperature, and then the samples were heated at 2 K/min to 400 °C in air to decompose the foam, and then at 5 K/min to 600 °C; they were kept at this temperature for 1 h to densify the glass filaments.

(2) In vitro bioactivity studies

(a) *Biomineralization assessment*

The *in vitro* biomineralization of the bioglass scaffolds was assessed by immersing the scaffolds in simulated body fluid (SBF) with a starting temperature at 37 °C for 5 and 10 days, the composition of the SBF was identical to that described by Kokubo *et al.* [23]. Crystalline phases formed on the surface of the glass scaffolds were determined by means of X-ray diffraction (XRD, Model D/MAX2200PC, Japan). XRD analysis was performed using Cu K_α radiation ($\lambda = 1.5406$ Å) at 40 kV and 30 mA, respectively. 2θ diffraction angle range was 10° – 70° with a step of 0.01° and a scanning rate of 0.5°/min. Phase identification was based on the ICDD PDF-4+ 2024 database (JCPDS 72 – 1243 for HA). Cross-section and topography of the surface of the glass scaffolds were observed with a scanning electron microscopy (SEM, S4800 Hitachi, Tokyo, Japan) at an accelerating voltage of 3.0 kV.

The compressive strength of cylindrical samples (6 mm in diameter × 10 mm) was measured using an Instron testing machine (Model 5566, UK) by applying 0 – 350 N axial load via a 500 N load cell at a crosshead speed of 0.5 mm/min, according to GB/T 10700 – 2006 Standard (China), respectively. The strain at which the voids begin to form was defined as the strain threshold. Glass is typically brittle and exhibits no yielding phenomenon so we took the maximum elastic deformation as the strain threshold in this study. The compressive strength of each scaffold was determined from the maximum load recorded during the test divided by the measured initial scaffold cross-sectional area of the specimen. Eight samples were tested, and the mean strength and standard deviation were determined. The porosity of the as-made glass scaffolds was measured with the Archimedes method.

For bioactivity studies, each scaffold (size: 1 cm × 1 cm × 1 cm) was immersed in 50 mL of SBF and stored in an oven at a controlled temperature of 37 °C. The SBF sample was renewed at various time periods (1, 3, 5, 8, 15, 20 days) up to 20 days. Ion changes of B were determined by means of inductively coupled plasma atomic emission spectrometry (ICP-AES, Spectra AA 220FS, THEM, USA) at 27.12 MHz frequency and 167 nm to 800 nm wavelength range. Ar gas was used during measurements. The study was repeated three times, and six replicates were used within each group.

(b) *Culture of human osteosarcoma cells and MTT detection*

The use of human osteosarcoma cells line MG-63 in this study was approved by the Fourth Military Medical University, Shaanxi, China. The MG-63 cells were cultured in a-MEM medium supplemented with 10 % fetal bovine serum plus 100 μg/ml penicillin and 100 μg/ml streptomycin sulfate. Before cell seeding, scaffolds measuring 6 mm in diameter and 2 mm in thickness, which had been sterilized using dry heat, were immersed for one hour in a 0.01 % polylysine solution (molecular weight exceeding 150 000) to improve cell adhesion. Following this pretreatment, the scaffolds were gently blotted to remove excess liquid and rinsed twice with phosphate-buffered saline (PBS). They were then positioned on a Teflon disk with a diameter of 6 cm and seeded with 50 000 MG-63 cells suspended in 35 μL of complete culture medium. To facilitate cell attachment, the seeded scaffolds were incubated for four hours. After this

period, the scaffolds were transferred to a 24-well plate, with each well containing 2 mL of complete medium. A control group was established by seeding the same number of cells directly into wells filled with 2 mL of complete medium, without the presence of scaffolds. All cell cultures were maintained at 37 °C in a humidified environment with 5 % CO_2, and the medium was replaced daily to ensure optimal cell growth conditions.

Cell adhesion on the surface of the glass scaffolds was investigated by means of SEM after 1 and 3 days of culture. At selected culture intervals, glass scaffolds with attached cells were removed, washed twice with warm PBS and placed in 2.5 % glutaraldehyde in PBS. After an overnight soak in glutaraldehyde, the glass samples were washed repeatedly with PBS, and then dehydrated with a graded ethyl alcohol series soaked for 10 min. Once naturally dry, the samples were sputter-coated with Au, and observed in an SEM at 5 kV accelerating voltage.

Cell proliferation was evaluated using the MTT test after 1 and 3 days of culture. Some of the cell-seeded scaffolds were placed in 400 µL serum-free medium containing 100 µg of the tetrazolium salt MTT for the last 4 h of incubation to permit visualization of metabolically active cells on and within the porous glass scaffolds. After the incubation, the scaffolds were briefly rinsed in PBS. 200 µL of dimethyl sulfoxide (DMSO; Sigma, USA) was added into each well and oscillated for 10 min. Finally, 200 µL of DMSO solution from each well was transferred to a 96-well plate, and the absorbance was measured at 570 nm in a multifunctional microplate reader (Wellscan MK3). The study was repeated three times, and six replicates were used within each study (n = 3). The data are presented as the mean ± standard deviation. Statistical analysis was performed using Student's t-test. Values were considered to be significantly different when $p < 0.05$.

(c) ***Structure assessment***

To determine the change in the glass structure when the CaO was substituted with SrO, glass samples were analyzed with Fourier Transform Infrared Spectroscopy (FTIR, Bruker VECTOR-22) in the wavenumber range of 4000 – 400 cm^{-1} using the KBr pellet method and a Bruker InfinityPlus 400 nuclear magnetic resonance (NMR) spectroscopy system. ^{11}B MAS-NMR spectra were acquired at a magnetic field strength of 9.4 T (Larmor frequency: 128.38 MHz) with a 4-mm probe, spinning rate of 12 kHz, and referenced to $BF_3{\cdot}Et_2O$ at 0 ppm.

III. Results and Discussion

(1) Degradation of glass scaffolds in SBF

XRD patterns of sample S_2 before and after soaking 5 and 7 days in SBF are shown in Fig. 1. The pattern of the as-formed scaffold shows broad bands of a typical amorphous material. After immersion for 5 days in SBF, the pattern of the scaffold contained peaks corresponding to those of a standard HA (JCDPS 72 – 1243), indicating the glass scaffolds exhibit good bioactivity. When the samples were immersed in SBF for 10 days, a well-crystallized HA phase could be found, which may be related to the further degradation of the glass phase and the gradual enrichment of the HA phase in the sample. HA is chemically and structurally equivalent to the main mineral components of bone, it is a key factor in the formation of a strong interfacial bond between the bioglass and tissues in the human body. The formation of a well-crystallized HA phase *in vitro* indicates that the prepared borate-based bioglass has the potential to be a good bone repair material.

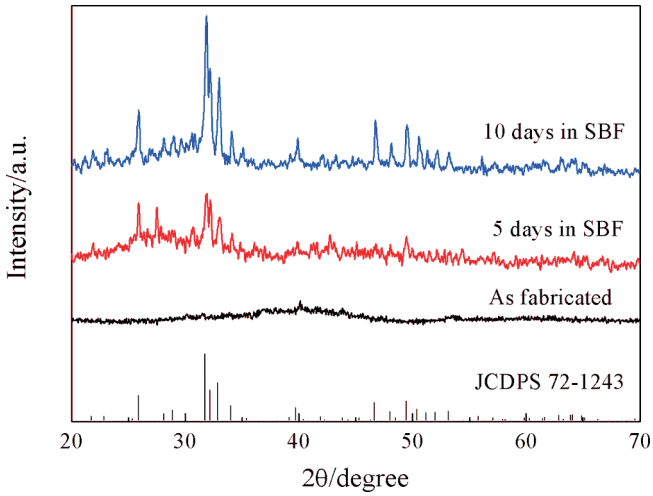

Fig. 1: X-ray diffraction of sample S_2 before and after soaking for 5 and 10 days in SBF.

Earlier studies indicated that a scaffold should have a porosity and compressive strength in the range of 50 – 90 % and 2 – 12 MPa in order to be used in tissue engineering applications as trabecular bone [24]. High porosity is important for cell proliferation. However, some scaffolds with a better degradation rate should have lower porosity than 90 % as they should preserve their microstructure until the new bone replacement [25]. The microstructure of a fractured cross-section of the glass scaffold is shown in Fig. 2a and b. We find that it consists of a dense network of glass and interconnected cellular pores. The porosity of all samples was about 85 %, and the compressive strength was greater than 11 MPa, which was close to the maximum value of human trabecular bone.

Figs. 2c and d show an SEM image of sample S_2 after it had been soaked in SBF solution for 5 and 10 days, respectively. Compared with the as-prepared smooth surface shown in Fig. 2a, a particle layer appeared on the surface of the glass soaked in SBF for 5 days, the particle size was 0.5 – 1.0 µm. It can be seen from Fig. 1 that the particles are HA. The HA particles only occupy a part of the glass surface, which also explains the reason why the diffraction peak of HA is not obvious when the soaking time is 5 days in Fig. 1. Fig. 2d shows a SEM image of the surface of the sample after it had been soaked in SBF solution for 10 days. It can be seen that the glass surface has been completely covered with HA, and the size of the HA particles is between 3 – 4 µm. The size, morphology and chemical composition of the HA crystals are similar to those of human trabecular bone. The rapid formation of the HA layer is a sign of high biomineralization activity, which is very beneficial for the application of bioactive implants in bone repair and bone regeneration [26].

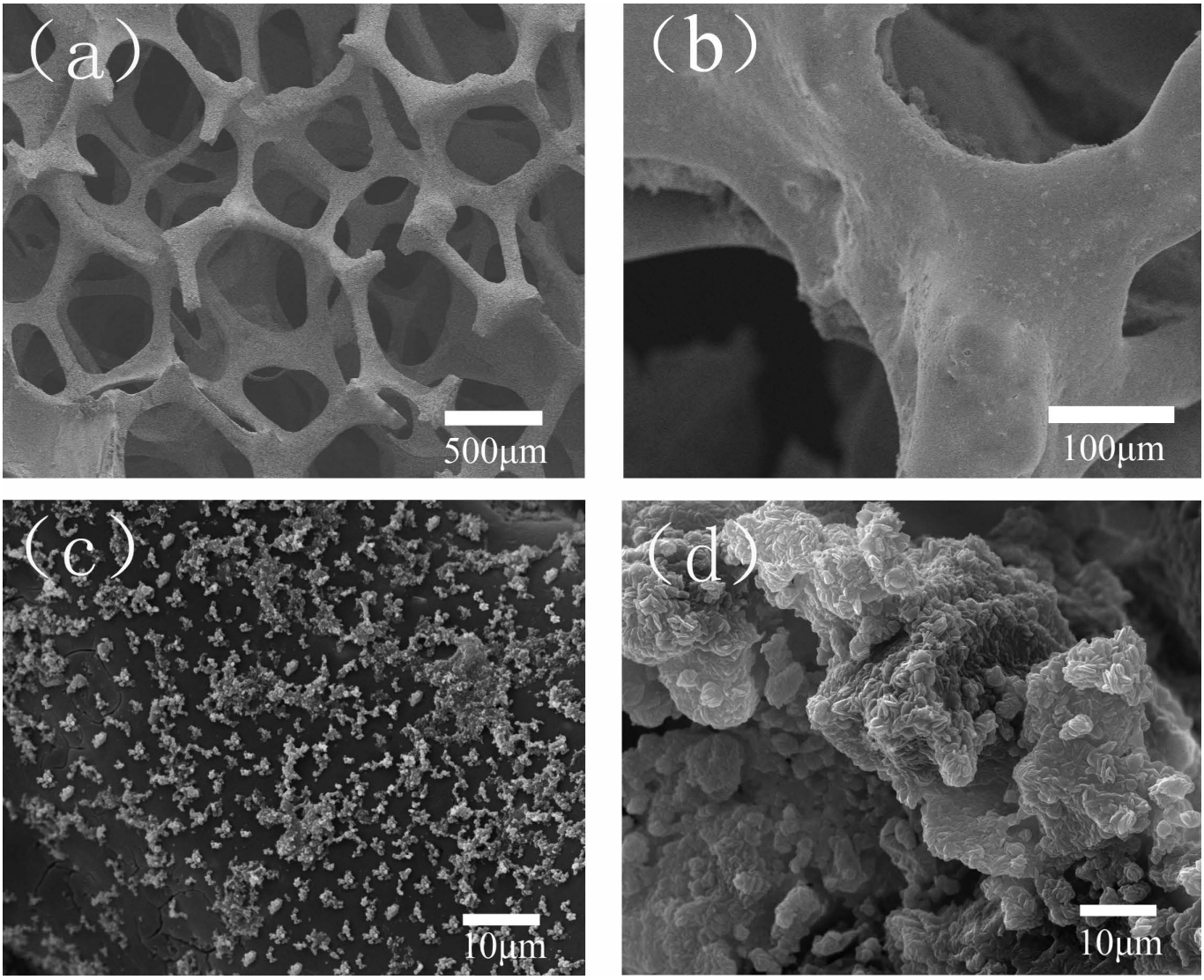

Fig. 2: SEM images of: (a), (b) sample S_2 fabricated with a polymer foam replication method; (c) 5 days in SBF; (d) 10 days in SBF.

Boron plays a crucial role in maintaining bone health, however, its cytotoxic effects are highly dependent on its concentration. According to Fu *et al.*, concentrations of boron exceeding 7 ppm have been shown to inhibit cellular growth and proliferation [20]. Fig. 3 illustrates the variations in B^{3+} ion concentrations before and after the scaffolds were immersed in simulated body fluid (SBF) for periods of 1, 3, 5, 8, 15 and 20 days. The concentration of B^{3+} ions in the SBF exhibited a significant increase during the initial 8 days, followed by a stabilization trend from the 15th to the 20th day. The rapid rise in the B^{3+} ion concentration at the onset of the experiment suggests that the silica network within the glass scaffolds dissolved at a faster rate, indicating the early formation of hydroxyapatite (HA) on the scaffold surfaces. By the 15th day, the B^{3+} ion concentration in the SBF began to stabilize, which can be attributed to the formation of $Si(OH)_4$ on the scaffold surfaces, marking the second phase of HA formation. What is more, with the substitution of strontium in glass scaffolds, the concentration of B^{3+} ions was reduced significantly (B^{3+} ions concentration of sample S_0 at the end of 20th day was 680 ppm, and sample S_1 was 620 ppm at the same time). The substitution of strontium in borate-based bioglass effectively inhibits the movement and release of boron, and keeps the B^{3+} ions concentration in a more acceptable [GS2] range to a certain extent.

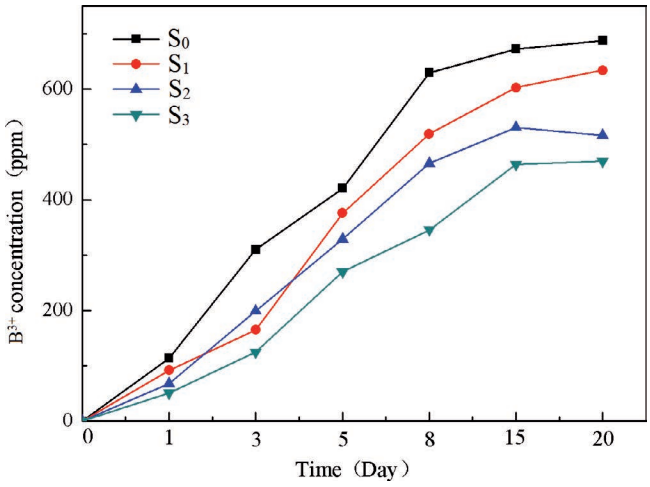

Fig. 3: B^{3+} ions changes of concentration after immersion in SBF for various time periods (1, 3, 5, 8, 15 and 20 days).

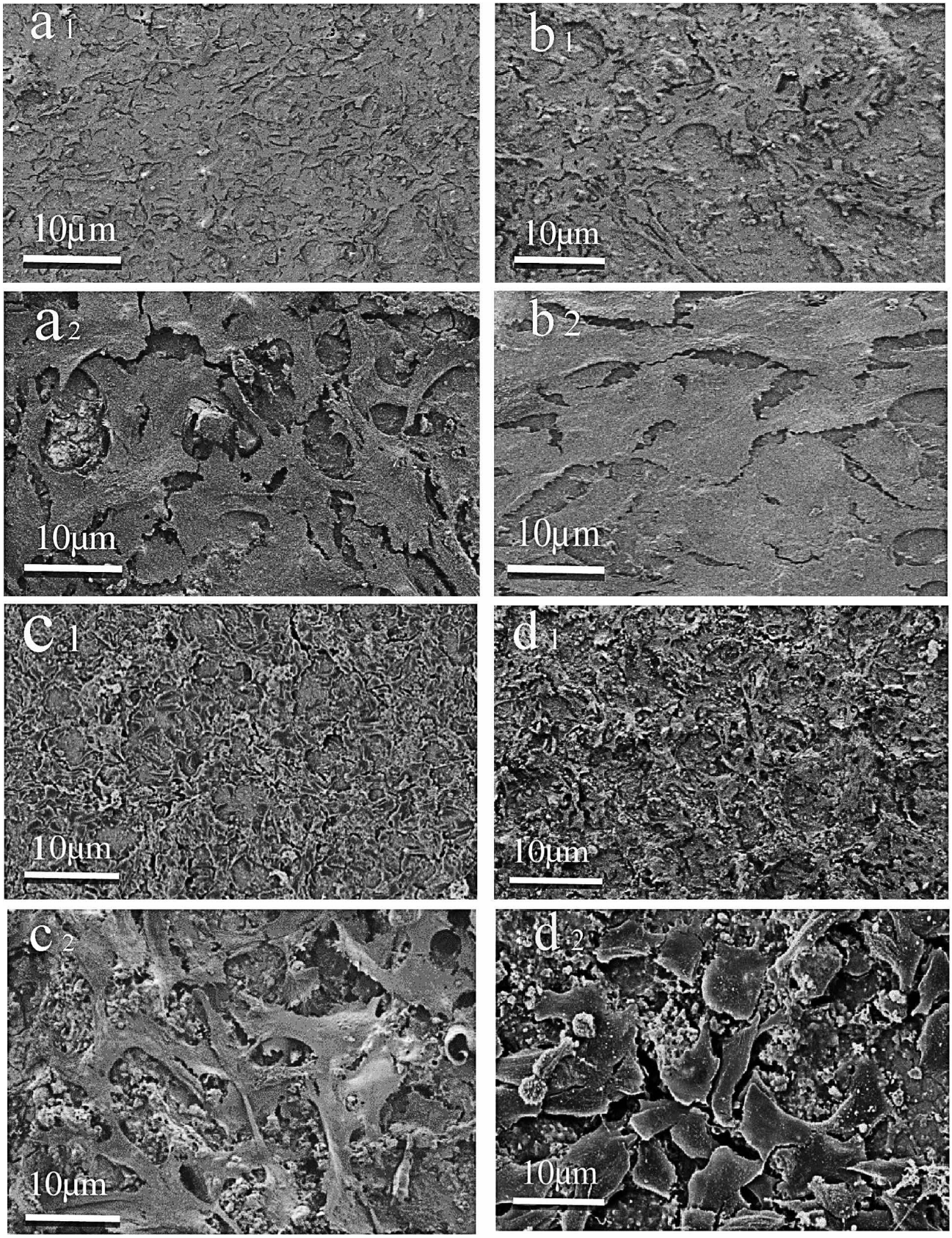

Fig. 4: SEM images of borate-based bioglass substitute by 0, 3, 6, 9 mol% SrO and seeded with MG-63 cells cultured for 1 day (a_1, b_1, c_1, d_1) and 3 days (a_2, b_2, c_2, d_2).

(2) Cell proliferation studies

Furthermore, we studied the effect of strontium substitution on cell adhesion and proliferation. Fig. 4 showed the SEM images of borate-based bioglass with 0, 3, 6, 9 mol% SrO substitution and seeded with MG-63 cells cultured for 1 and 3 days. As can be seen from Figs. 4 a_1, b_1, c_1, and d_1, on the first day, the cells were well attached to the bioglass surface and had some lamellae and cell protrusions. As

the amount of strontium substitution increased, the cell density increased. Compared with the first day, it can be seen in Figs. 4 a_2, b_2, c_2, and d_2 that MG-63 cells on the third day appeared colonized on the surface of the borate-based bioglass scaffold with 1 – 2 μm gaps, neighboring cells maintain physical contact and aggregate with neighboring cells through multiple extensions. Comparing the first and third days, we found that the cells showed good adhesion and diffusivity on the surface of bioglass, and borate-based bioglass significantly promoted the adhesion of MG-63 cells. In certain ranges, this promotion increases as the amount of strontium substitution increases.

The result of MTT assay on MG-63 cells with borate-based bioglass is shown in Fig. 5. On the first day, compared with control group, the MG-63 cells proliferation of sample S_0 showed no obvious difference. However, the substitution of strontium elevated the proliferation of MG-63 cells significantly ($p < 0.05$). On day 3, 13 – 93B2 glass scaffolds clearly inhibited cell proliferation, and the proliferation of other samples was further improved with the appearance of strontium. The MTT assay provided further evidence that strontium substitution in 13 – 93B2 glass suppressed the rapid release of boron and the cytotoxicity of glass scaffolds could at least be minimized.

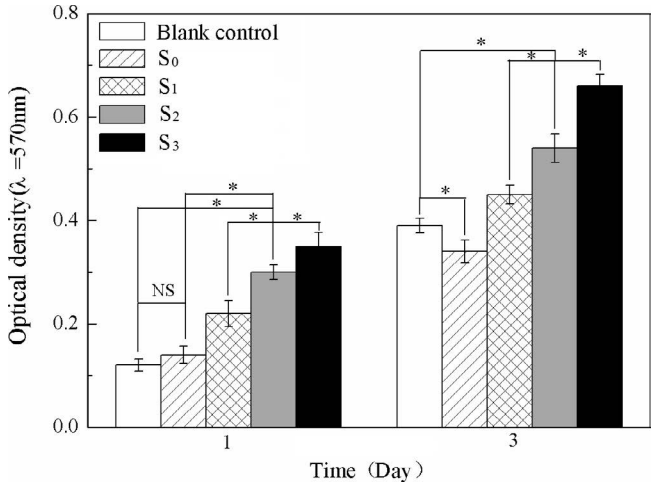

Fig. 5: Proliferation of MG-63 cells cultured with the scaffolds for 1 and 3 days, data were represented as mean ± SD, n=3; differences were considered significant when *$P < 0.05$.

(3) Structural studies

An FTIR spectrum of bioglass samples after soaking for 5 days in SBF is shown in Fig. 6. The graph shows two characteristic bands of silicates at 1 065 cm^{-1} and 479 cm^{-1}, The bands in the range 470 – 512 cm^{-1} were attributed to the bending mode of Si-O. The bands in the range 1 050 – 1 100 cm^{-1} were related to P-O-Si stretching vibrations. The peak appearing at 570 cm^{-1} is due to the bending vibration of P-O in [PO_4]. The peaks appearing at 690 cm^{-1} and 1 430 cm^{-1} are related to the bending vibration of B-O and the stretching vibration of C-O. The peaks of 1 600 cm^{-1} and 3 600 cm^{-1} correspond to the stretching vibration and bending vibration of O-H.

It can be found that as the amount of strontium substitution in the bioglass increases, the bending vibration peak of P-O at 570 cm^{-1} gradually decreases. The characteristic peak of Si-O at 1 065 cm^{-1} showed the same trend, however, the characteristic peak of C-O at 1 430 cm^{-1} is gradually enhanced. The reason for this phenomenon is a change in the glass structure owing to the substitution of strontium. As reported in some papers, Sr will take the position of Ca in the glass network, and Sr has a larger atomic radius than Ca, disrupting part of the silicate network structure and making the glass structure more open [21]. When the bioglass samples were immersed in SBF, $(PO_4)^{3-}$ and related ions were gradually released to form HA, while the glass network structure was gradually degraded and destroyed, thus the characteristic peaks of Si-O and P-O gradually weaken. The enhancement of the characteristic peak of the C-O bond is associated with the gradual increase of carbonized HA formed by the mineralization of bioglass.

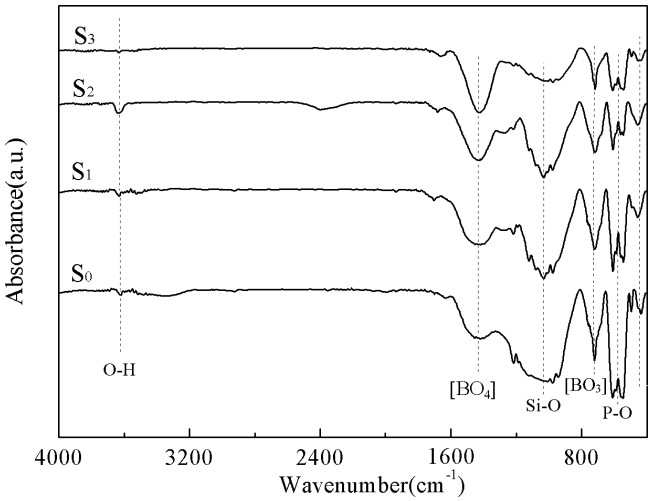

Fig. 6: FTIR spectra of bioglass samples after soaking for 5 days in SBF.

B^{11} MAS-NMR analysis was employed to quantify the presence of tricoordinated B^{III} ions and tetracoordinated B^{IV} ions within the samples by measuring the energy-level differences of boron ions during energy-level transitions under a strong magnetic field. The concentrations of these ions are represented by the peak intensities observed in the spectrum. As illustrated in Fig. 7, a prominent peak corresponding to boron ions is observed at 20 ppm, which further splits into two distinct peaks at 9 ppm and 15 ppm. Based on the findings of Zhao *et al.*, the peak at approximately 9 ppm is indicative of B^{IV} ions, which predominantly constitute the [BO_4] structural units, while the peak at 15 ppm is characteristic of B^{III} ions, primarily associated with [BO_3] units [28]. From the spectral data, it is evident that as the SrO content increases, the concentration of B^{III} ions progressively diminishes, whereas the concentration of B^{IV} ions shows a corresponding increase. This observation suggests that the incorporation of SrO induces structural modifications in the borate-based bioglass, leading to a gradual transformation from a layered structure dominated by [BO_3] units to a framework structure primarily composed of

[BO_4] units. Consequently, these structural changes result in alterations to certain properties of the glass, often in opposing directions. In summary, we controlled the dissolution rate of B^{3+} in a proper [GS3] range by changing glass structure, at the same time, the bioactivity properties of borate-based bioglass improved.

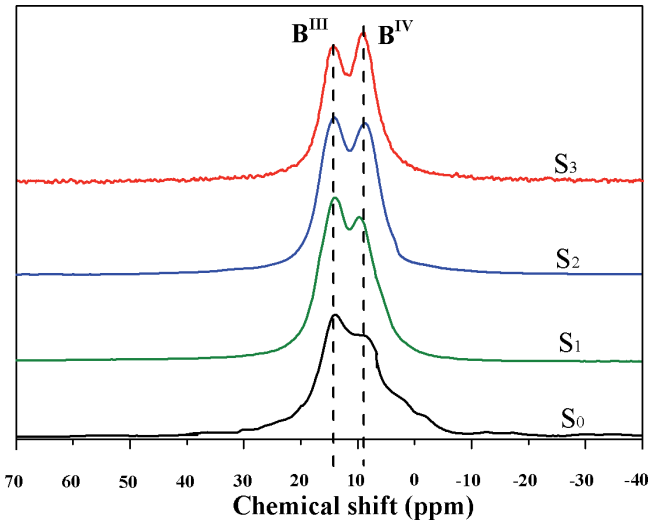

Fig. 7: B^{11} MAS-NMR spectra of the borate-based bioglass with different SrO concentrations.

IV. Conclusions

In the research described in this paper, strontium substitution of borate-based bioglass was effected with a polymer foam replication method. From the results of XRD and SEM analysis, it has been proved that the as-fabricated bioglass was amorphous and composed of a dense network microstructure. After the bioglass scaffolds had been immersed in SBF for five days, a nanostructured hydroxyapatite layer formed on bioglass surface, on the tenth day, the surface was completely covered by HA. *In vitro* studies showed that the concentration of B^{3+} ions was reduced significantly with the substitution of strontium in the bioglass. Cell culture experiments showed that MG63 cells exhibited good adhesion and proliferation ability on bioglass surfaces, and the presence of strontium in borate-based bioglass suppressed the rapid release of boron so that the cytotoxicity of glass scaffolds could at least be minimized. Then, the change of the structure of strontium substitution of borate-based bioglass was studied by FTIR and MAS-NMR tests. We found that Sr will take the position of Ca in the glass network and destroy part of the silicate network structure, making the glass structure more open. At the same time, the substitution of SrO results in some changes to the structure of borate-based bioglass, and the layer structure containing [BO_3] gradually replaced by the framework structure containing [BO_4], led to improved bioactivity properties of borate-based bioglass.

References

1 De Silva, L., Bernal, P.N., Rosenberg, A.J.W., Malda, J., Levato, R., Gawlitta, D.: Biofabricating the vascular tree in engineered bone tissue, *Acta. Biomater.,* **156**, 250 – 268, (2023).

2 Hench, L.L.: Bioceramics: from concept to clinic, *J. Am. Ceram. Soc.,* **74**, 1487 – 1510, (1991).

3 Chunyan, T., Kun, L., Fuhuan, C., Qiujiang, W., Shiqi, X., Linhui, Q., Xinrui, G.: Preparation and performance study of *in situ* mineralized bone tissue engineering scaffolds, *RSC Adv.,* **14**, 22420 – 22433, (2024).

4 Tadashi, K.: Bioactive glass ceramics: properties and applications, *Biomaterials,* **12**, 155 – 163, (1991).

5 Youness, R.A., Al-Ashkar, E., Taha, M.A.: Role of porosity in the strength, dielectric properties, and bioactivity of hardystonite ceramic material for use in bone tissue engineering applications, *Ceram. Int.,* **49**, 40520 – 40531, (2023).

6 Siekkinen, M., Karlström, O., Hupa, L.: Effect of local ion concentrations on the in vitro reactions of bioactive glass 45S5 particles, *Int. J. Appl. Glass Sci.,* **13**, 695 – 707, (2022).

7 Hench, L.L., Splinter, R.J., Allen, W.C., Greenlee, T.K.: Bonding mechanisms at the interface of ceramic prosthetic materials, *J. Biomed. Mater. Res.,* **5**, 117 – 141, (1971).

8 Kowalska, K.J., Czechowska, J.P., Yousef, E.-S., Zima, A.: Novel phosphate bioglasses and bioglass-ceramics for bone regeneration, *Ceram. Int.,* **50**, 45976 – 45985, (2024).

9 Yoo, K.-H., Son, S.-A., Park, J.K., Yoon, S.-Y.: Influence of glass composition on the network structure and mineralization of europium containing mesoporous bioactive glass nanoparticles, *Mater. Chem. Phys.,* **317**, 1 – 7, (2024).

10 Nommeots-Nomm, A., Hupa, L., Rohanová, D., Brauer, D.S.: A review of acellular immersion tests on bioactive glasses-influence of medium on ion release and apatite formation, *Int. J. Appl. Glass. Sci.,* **11**, 537 – 551, (2020).

11 Zhang, X., Guo, X., Zhang, J., Fan, X., Chen, M., Yang, H.: Nucleation, crystallization and biological activity of Na_2O-CaO-P_2O_5-SiO_2 bioactive glass, *J. Non-Cryst. Solids.,* **568**, 1 – 7, (2021).

12 Hung, G-Y., Chen, P.-Y., Wang, C.-Y., Tu, C.-S., Chen, C.-S., C., Lai, P.-L., L., Feng, K.-C.: Tailoring bioactive and mechanical properties in polycrystalline CaO-SiO_2-P_2O_5 glass-ceramics, *Ceram. Int.,* **49**, 7289 – 7298, (2023).

13 Shearer, A., Montazerian, M., Sly, J.J., Hill, R.G., Mauro, J.C.: Trends and perspectives on the commercialization of bioactive glasses, *Acta Biomater.,* **160**, 14 – 31, (2023).

14 Yusof, N.N., Aziz, S.M., Mohd Noor, F., Syed Yaacob, S.N., Hashim, S.: A novel borate-based 45S5 Bioglass®: *In vitro* assessment in phosphate-buffered saline solution, *J. Non-Cryst. Solids.,* **596**, 1 – 14, (2022).

15 Wen, C., Xie, M., Yan, S., Chen, Q., Jin, J., Xie, T., Zhu, W., Tang, Z., Luo, K., Sa, B.: Effects of B_2O_3 on the structural evolution and biological behavior of borate bioactive glasses by sol-gel and melting methods, *Ceram. Int.,* **50**, 47864 – 47875, (2024).

16 Ouis, M.A., Abdelghany, A.M., Elbatal, H.A.: Corrosion mechanism and bioactivity of borate glasses analogue to Hench's bioglass, *Process. Appl. Ceram.,* **6**, 141 – 149, (2012).

17 Fakhar, S., Westenberg, D.: Borate-based bioactive glasses properties: clinical and biomedical applications, *Ceram. Int.,* **50**, 52190 – 52204, (2024).

18 Tan, R., Chen, R., Sun, L., Xu, S., Ji, Z., Ji, S., Liu, C., Zhao, X., Xu, H., Xia, H., Wang, Y., Wang, J., Ma, K.: From nanoscale to microscale hierarchical multifunctional nano borate bioactive glass for efficient wound healing, *Ceram. Int.,* **49**, 25908 – 25919, (2023).

19 Zhou, J., Wang, H., Zhao, S., Zhou, N., Li, L., Huang, W., Wang, D., Zhang, C.: In vivo and in vitro studies of borate based glass micro-fibers for dermal repairing, *Mater. Sci. Eng. C.,* **60**, 437 – 445, (2016).

[20] Fu, H., Fu, Q., Zhou, N., Huang, W., Rahaman, M.N., Wang, D., Liu, X.: In vitro evaluation of borate-based bioactive glass scaffolds prepared by a polymer foam replication method, *Mater. Sci. Eng. C.,* **29**, 2275 – 2281, (2009).

[21] Fujikura, K., Karpukhina, N., Kasuga, T., Brauer, D.S., Hill, R.G., Law, R.V.: Influence of strontium substitution on structure and crystallisation of Bioglass® 45S5, *J. Mater. Chem.,* **22**, 7395 – 7402, (2012).

[22] Fu, Q., Rahaman, M.N., Sonny Bal, B., Brown, R.F., Day, D.E.: Mechanical and in vitro performance of 13 – 93 bioactive glass scaffolds prepared by a polymer foam replication technique, *Acta Biomater.,* **4**, 1854 – 1864, (2008).

[23] Kokubo, T., Kushitani, H., Sakka, S., Kitsugi, T., Yamamuro, T.: Solutions able to reproduce in vivo surface-structure changes in bioactive glass-ceramic A-W3, *J. Biomed. Mater. Res.,* **24**, 721 – 734, (1990).

[24] Darus, F., Isa, R.M., Mamat, N., Jaafar, M.: Techniques for fabrication and construction of three-dimensional bioceramic scaffolds: effect on pores size, porosity and compressive strength, *Ceram. Int.,* **44**, 18400 – 18407, (2018).

[25] Fu, Q., Saiz, E., Tomsia, A.P.: Bioinspired strong and highly porous glass scaffolds, *Adv. Funct. Mater.,* **21**, 1058 – 1063, (2011).

[26] Lomelino, R.D.O., Castro-Silva, I.I., Linhares, A.B.R., Gutemberg G.A., de Albuquerque Santos, S.R., Gameiro, V.S., Rossi, A.M., Granjeiro, J.M.: The association of human primary bone cells with biphasic calcium phosphate (βTCP/HA 70:30) granules increases bone repair, *J. Mater. Sci.:Mater. Med.,* **23**, 781 – 788, (2012).

[27] Fernando, D., Attik, N., Pradelle-Plasse, N., Jackson, P., Grosgogeat, B., Colon, P.: Bioactive glass for dentin remineralization: A systematic review, *Mater. Sci. Eng. C.,* **76**, 1369 – 1377, (2017).

[28] Zhao, P., Kroeker, S., Stebbins, J.F.: Non-bridging oxygen sites in barium borosilicate glasses: results from 11B and 17O NMR, *J. Non-Cryst. Solids.*, **276**, 122 – 131, (2000).